NASA/CR—2019–220229

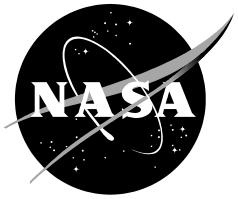

Experimental Forward Flight Rotor Performance Testing From Terrestrial to Martian Atmospheric Densities

Brenda Natalia Perez Perez, Geoffrey A. Ament, and Witold J. F. Koning
Science and Technology Corporation
Ames Research Center, Moffett Field, California

June 2019

NASA STI Program ... in Profile

Since its founding, NASA has been dedicated to the advancement of aeronautics and space science. The NASA scientific and technical information (STI) program plays a key part in helping NASA maintain this important role.

The NASA STI program operates under the auspices of the Agency Chief Information Officer. It collects, organizes, provides for archiving, and disseminates NASA's STI. The NASA STI program provides access to the NTRS Registered and its public interface, the NASA Technical Reports Server, thus providing one of the largest collections of aeronautical and space science STI in the world. Results are published in both non-NASA channels and by NASA in the NASA STI Report Series, which includes the following report types:

- TECHNICAL PUBLICATION. Reports of completed research or a major significant phase of research that present the results of NASA Programs and include extensive data or theoretical analysis. Includes compilations of significant scientific and technical data and information deemed to be of continuing reference value. NASA counterpart of peer-reviewed formal professional papers but has less stringent limitations on manuscript length and extent of graphic presentations.

- TECHNICAL MEMORANDUM. Scientific and technical findings that are preliminary or of specialized interest, e.g., quick release reports, working papers, and bibliographies that contain minimal annotation. Does not contain extensive analysis.

- CONTRACTOR REPORT. Scientific and technical findings by NASA-sponsored contractors and grantees.

- CONFERENCE PUBLICATION. Collected papers from scientific and technical conferences, symposia, seminars, or other meetings sponsored or co-sponsored by NASA.

- SPECIAL PUBLICATION. Scientific, technical, or historical information from NASA programs, projects, and missions, often concerned with subjects having substantial public interest.

- TECHNICAL TRANSLATION. English-language translations of foreign scientific and technical material pertinent to NASA's mission.

Specialized services also include organizing and publishing research results, distributing specialized research announcements and feeds, providing information desk and personal search support, and enabling data exchange services.

For more information about the NASA STI program, see the following:

- Access the NASA STI program home page at http://www.sti.nasa.gov

- E-mail your question to help@sti.nasa.gov

- Phone the NASA STI Information Desk at 757-864-9658

- Write to:
  NASA STI Information Desk
  Mail Stop 148
  NASA Langley Research Center
  Hampton, VA 23681-2199

NASA/CR—2019–220229

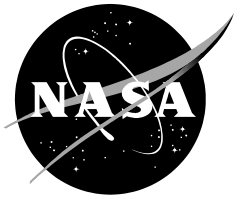

Experimental Forward Flight Rotor Performance Testing From Terrestrial to Martian Atmospheric Densities

Brenda Natalia Perez Perez, Geoffrey A. Ament, and Witold J. F. Koning
Science and Technology Corporation
Ames Research Center, Moffett Field, California

National Aeronautics and
Space Administration

Ames Research Center
Moffett Field, CA 94035-1000

June 2019

ACKNOWLEDGMENTS

The authors would like to thank Farid Haddad for his expertise in electronics and controls during experimental setup, Ken Smith for operation of the PAL vacuum facility, Eduardo Solis for scanning the 40x22 AWT rotor for RotCFD simulation, Larry Meyn for his expertise with the data reduction, Larry Young for originally inspiring the idea of forward flight testing under Martian conditions, Haley Cummings for her invaluable feedback and support throughout the project, and William Warmbrodt for his continued support and guidance on the project. Lastly, a thank you to the 2017–2018 Aeromechanics Interns for their support during data collection.

TABLE OF CONTENTS

TABLE OF CONTENTS (cont.)

LIST OF FIGURES

LIST OF TABLES

NOMENCLATURE

CFD	Computational Fluid Dynamics
DAS	Data Acquisition System
IR	infrared
JPL	Jet Propulsion Laboratory
MARSWIT	Martian Surface Wind Tunnel
MH	Mars Helicopter
PAL	Planetary Aeolian Laboratory
RAP	Resonance Assessment Profile
UAV	Unmanned Aerial Vehicle
point	Point number within a run during testing
run	Run number during testing
SVS	NASA Ames Thermal Physics Facility's Steam Vacuum System
C_{Mx} (~)	Roll moment coefficient
C_{My} (~)	Pitch moment coefficient
C_P (~)	Power coefficient
C_T (~)	Thrust coefficient
D (lbf)	Rotor drag force
FM (~)	Figure of merit
M_{tip} (~)	Advancing tip Mach number
Mx (in-lb)	Roll moment
My (in-lb)	Pitch moment
n (~)	Number of propellers fixed to the rotor shaft during testing
P (hp)	Power
P (millibar)	Chamber pressure in the PAL
Pi (hp)	Ideal power
Q (ft-lb)	Torque applied by the motor
Re.75 (~)	Reynolds number at a radial station of 0.75
RPM (~)	Revolutions per minute
S (lb)	Rotor side force
T (^{0}F)	Temperature in the PAL
T (lb)	Thrust measured by load cells
V (ft/s)	Free stream velocity
ν (ft^2/s)	Kinematic viscosity of air
φ (deg)	Azimuth angle of thrust vector location, measured counterclockwise from 0-degree azimuth
ρ (lb/ft^3)	Air density in the PAL

EXPERIMENTAL FORWARD FLIGHT ROTOR PERFORMANCE TESTING FROM TERRESTRIAL TO MARTIAN ATMOSPHERIC DENSITIES

Brenda Natalia Perez Perez, Geoffrey A. Ament, and Witold J. F. Koning[1]

Ames Research Center

SUMMARY

With the recent interest in Martian exploration using Unmanned Aerial Vehicles (UAVs), an experimental study was conducted to investigate rotor performance at Martian atmospheric conditions. Both simulation and testing of rotors are vital for the evaluation of rotor performance and behavior, especially for operations at Martian atmospheric densities and pressures. Testing and measuring rotor forward flight performance at Martian atmospheric conditions is a relatively unexplored area. Therefore, an experimental study was performed in a wind tunnel to investigate helicopter forward flight performance and to demonstrate successful rotor operation at Martian atmospheric densities. This work was a continuation of the first-ever wind tunnel test of a simulated rotorcraft in forward flight at Martian atmospheric densities. A test was conducted in a facility that could be evacuated to the atmospheric pressure and density of Mars. A 40-inch-diameter rotor, roughly approximating the scale of the proposed Mars Helicopter (MH) design by the NASA Jet Propulsion Laboratory (JPL), was tested in forward flight at Mars' atmospheric pressure at the NASA Ames Planetary Aeolian Laboratory (PAL). In this forward flight testing, the drive system of the Martian Surface Wind Tunnel (MARSWIT) was never turned on. The goal of this experiment was to collect rotor thrust, rotational speed, power, torque, and wind speed measurements. Subsequently, these results can be used for correlation with simulated cases using a mid-fidelity Computational Fluid Dynamics (CFD) simulation. Rotor thrust and power seem to decrease approximately proportional to the decrease in density. However, the Reynolds number has an effect on rotor performance that might also be contributing to the change in thrust and power. This effect plays a vital role in rotor performance at reduced pressure that cannot be neglected in the simulation. Despite the challenges involved in testing at a large difference of atmospheric densities between Earth and Mars, repeatable data is obtained in all the measurements at Martian atmospheric conditions.

INTRODUCTION

The work presented here is an extension of the initial study performed by Ament, Koning, and Perez Perez [1]. Information is repeated in this report for the benefit of the reader. However, sections have been modified to describe the distinctive aspects of this work.

[1] Science and Technology Corporation, NASA Research Park, Moffett Field, CA 94035.

In the interest of exploring and learning more about our solar system, NASA has performed several unmanned missions to Mars. Among these successes, various missions to Mars have allowed for close examination of the Martian surface, and one rover is still in operation today. Unfortunately, because of Mars' rocky terrain and communication delays between Earth and Mars, it can be difficult to efficiently move around on the Martian surface. In an effort to help resolve these issues, the NASA Jet Propulsion Laboratory (JPL) is developing a Mars Helicopter (MH) in collaboration with AeroVironment Inc., NASA Ames Research Center, and NASA Langley Research Center, to create a low-altitude Unmanned Aerial Vehicle (UAV) to scout in the vicinity of the rover and explore the red planet [2].

Considering the drastic differences in gravity and atmospheric conditions between Earth and Mars, many obstacles must be overcome when designing a flight vehicle for Martian exploration. Because the gravity on Mars is roughly one-third that of Earth's, a flight vehicle weighs less on Mars than on Earth; consequently, a flight vehicle would need less thrust to become airborne. However, the reduced thrust required from a lighter vehicle is undermined by the drastic reduction in atmospheric density, which is approximately 1 percent of Earth's atmospheric density. In addition, the reduction in temperature, specific heat ratio, and atmospheric gas constant reduce the speed of sound considerably. Further, the low Reynolds number for a rotor operating in a Martian atmosphere has a high impact on rotor performance because of possible early flow separation on the blade [3].

TEST FACILITY

Planetary Aeolian Laboratory

The Planetary Aeolian Laboratory (PAL) is a 98.5-foot-high, 141,259-cubic-foot-volume, near-vacuum facility capable of conducting experiments under atmospheric conditions ranging from Earth's atmosphere, approximately 1 bar, down to 5.5 millibars [4], which is less than the atmospheric pressure of Mars. The facility can be evacuated to its minimum pressure of 5.5 millibars in about 45 minutes, an operation performed by the NASA Ames Thermal Physics Facility's Steam Vacuum System (SVS) [4].

At all atmospheric conditions, the PAL chamber atmosphere composition is that of Earth's; for noncritical Mach numbers, differences between Earth's (primarily O_2 and N_2) and Mars' (primarily CO_2) atmosphere are thought to be negligible. That said, it is expected that the 100-fold change in density will completely offset the comparatively small change in viscosity, specific heat ratio, and gas constant due to the change of gas type. Because of the high cost to evacuate the PAL, the majority of the PAL testing is done in conjunction with other NASA Ames projects already requiring vacuum; in doing so, the windows of time allotted to PAL vacuum testing are often based on dual-use opportunities. Although not pursued for this project, vacuum testing can be dedicated to the PAL if sufficient funding is in place, allowing for extensive low-pressure testing. The PAL is shown in Figure 1.

Martian Surface Wind Tunnel

The Martian Surface Wind Tunnel (MARSWIT), shown in Figure 2, was first put into operation in 1976 and is an open-circuit 43-foot-long atmospheric boundary-layer wind tunnel. The

internal cross section is 3.3 feet high by 4 feet wide [5]. As the MARSWIT is in the PAL near-vacuum chamber, the wind tunnel can be tested at all atmospheric conditions of which the facility is capable; at 1 atmosphere the wind tunnel can reach wind speeds of 34.5 ft/s, and at 5 millibars, wind speeds of 328 ft/s. The tunnel has been used to investigate the physics of particle entrainment under Martian conditions, to test spacecraft instruments under Martian conditions [5], and recently to test rotor performance. All test data presented in this paper was acquired with the wind tunnel drive system turned off.

Figure 1. Planetary Aeolian Laboratory (PAL).

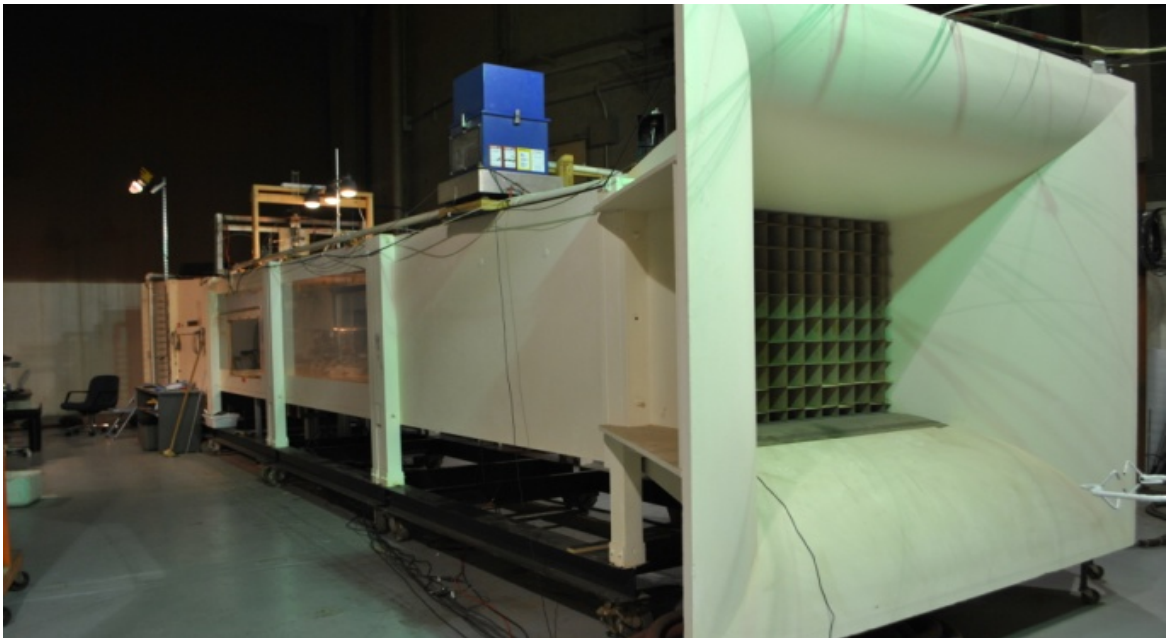

Figure 2. PAL Martian Surface Wind Tunnel.

TEST INSTALLATION, HARDWARE, AND DATA COLLECTION

Hardware Installation

Test hardware was installed into the MARSWIT test section, approximately located midway along the 43-foot-long wind tunnel. Testing consisted of both two-bladed and four-bladed rotor configurations. The two-bladed rotor was used to test a rotor in nominal helicopter mode. The four-bladed rotor resembled the MH's coaxial design, and provided increased rotor thrust representative of the MH design. However, unlike the MH's coaxial system, both rotors in the four-bladed configuration are fixed, rotating in the same direction, at 90-degree orientation. Both the two- and four-bladed rotor configurations are shown in Figure 3.

Test hardware was designed such that the rotor could be tested between ±14 degrees angle of attack. For the presented data, all tests were conducted at –14 degrees, pitching the test apparatus towards the tunnel inlet. Figure 4 shows the two-bladed rotor configuration at 0 and –14 degrees (forward flight). Figure 5 shows the rotor again at –14 degrees, but from downstream of the test section.

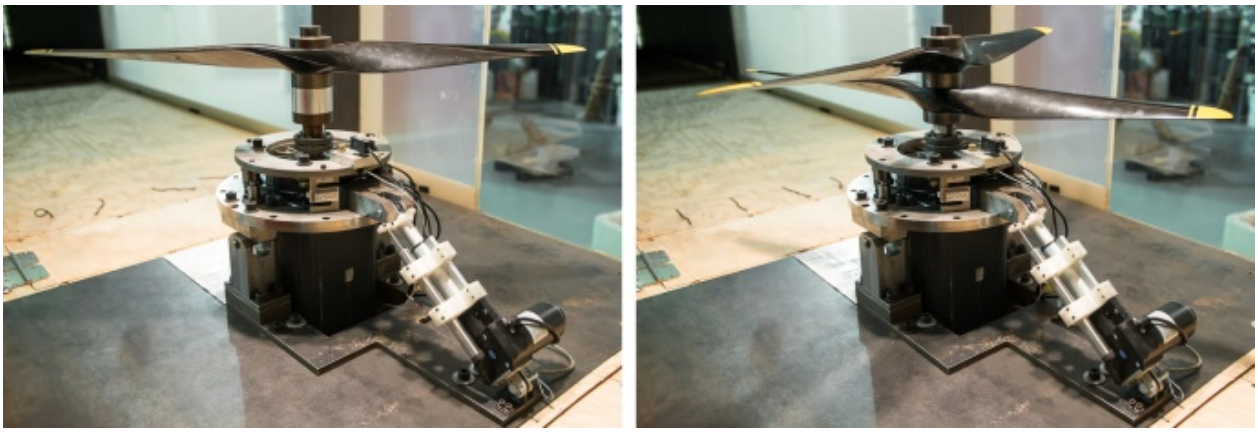

Figure 3. Left and right images show two- and four-bladed rotor configurations tested in the MARSWIT test section, respectively.

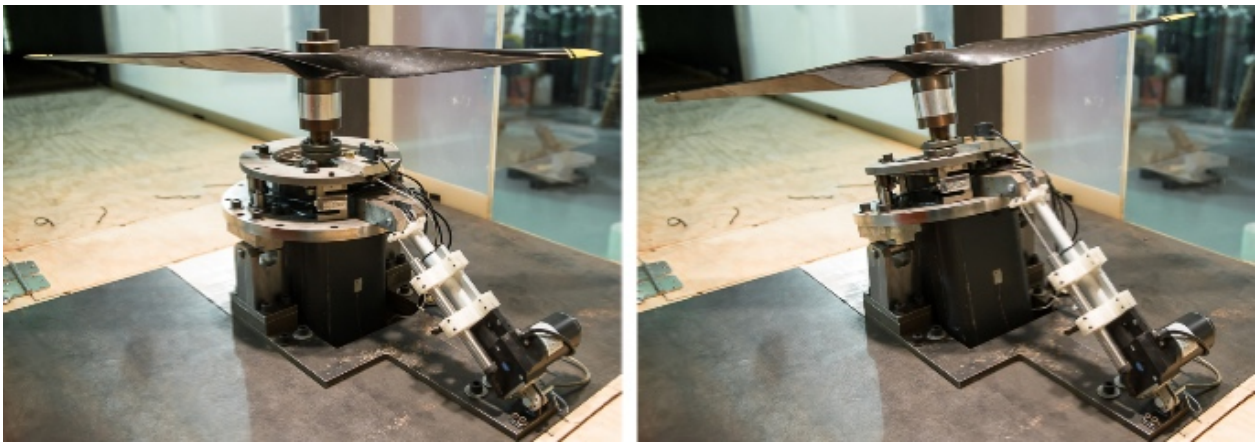

Figure 4. Left image shows two-bladed rotor at a 0-degree shaft angle; right image shows two-bladed rotor at a –14-degree shaft angle.

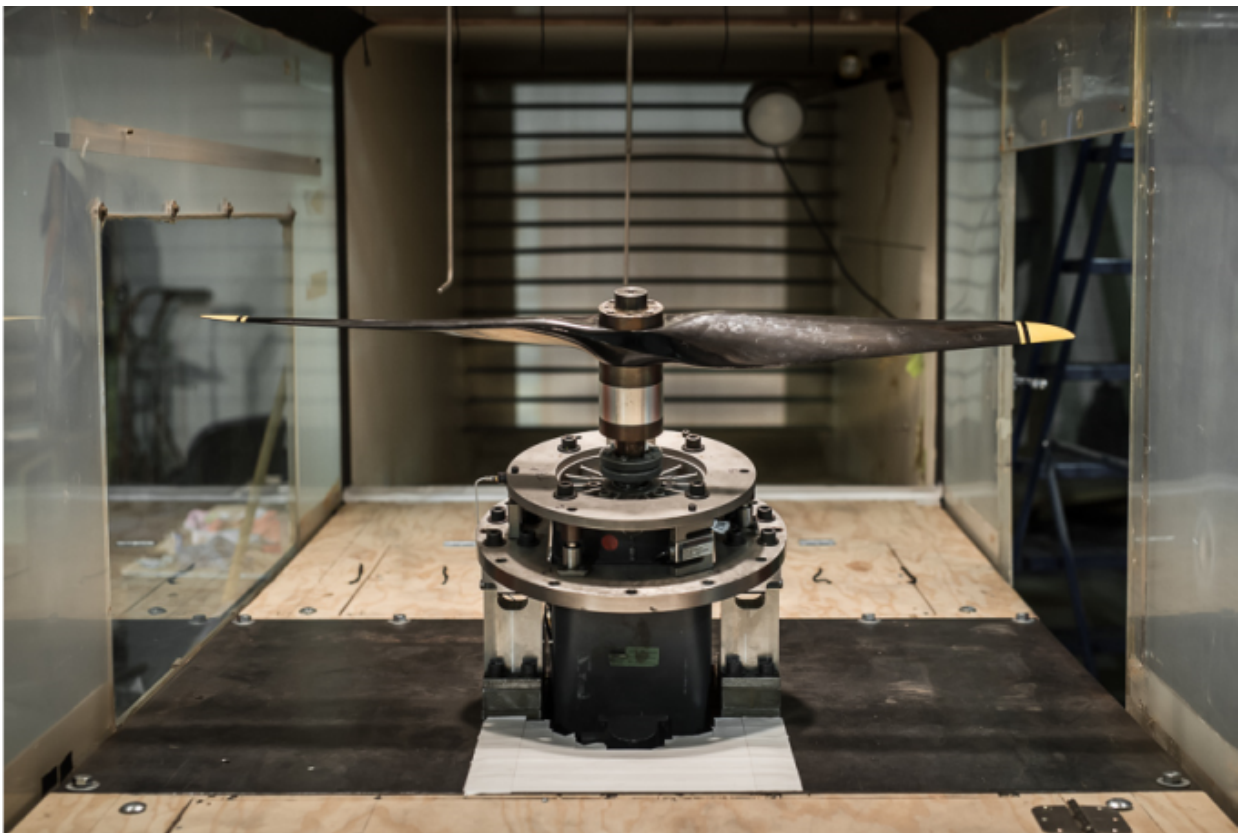

Figure 5. Two-bladed rotor at a –14-degree shaft angle, looking downstream of the test section.

Testing was conducted from a pressure range of 1 atmosphere (Earth's atmosphere) down to 5.5 millibars (conditions which approximate the atmospheric conditions found on Mars).

Test Hardware

The primary goals were to collect rotor thrust, RPM, power, torque, motor temperature, and wind speed, as well as chamber pressure, humidity, and temperature, while in forward flight. The following sections discuss the hardware and sensors used to obtain this data, and reference Figure 6 and Figure 7 for location within the MARSWIT.

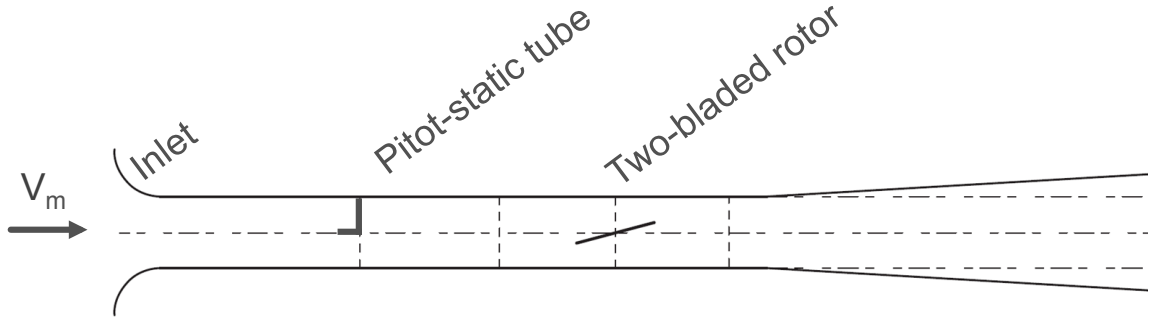

Figure 6. Side profile of the 43-foot-long MARSWIT.

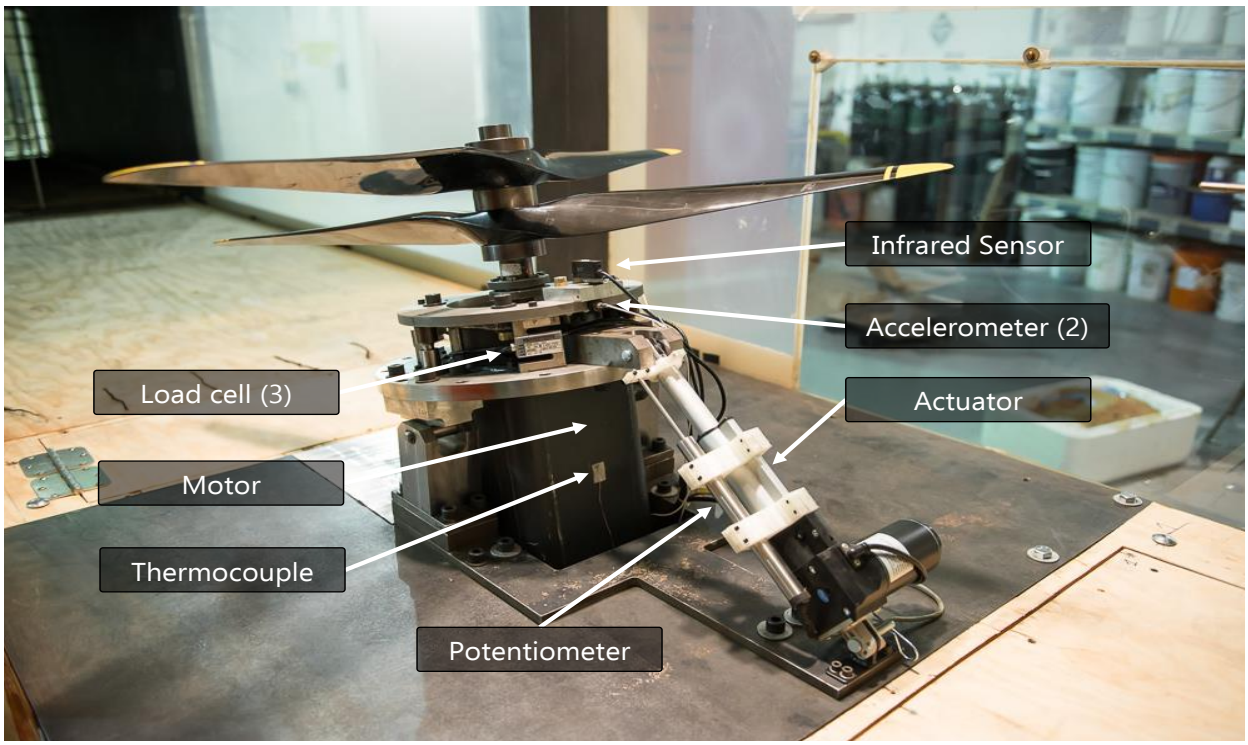

Figure 7. Hardware and sensor installation within the MARSWIT test section.

Prior to MH testing in the JPL 25-foot Space Simulator, a 1-atmosphere rotor hover safety checkout needed to be conducted within the chamber. As part of this effort, the 40x22 rotor was selected in 2015 and tested for this activity [6]. The same rotor blades and motor were used for reduced pressure forward flight testing at NASA Ames Research Center in 2017.

To provide a better understanding of what the MH might experience during forward flight on Mars, the selected rotor was chosen based on the physical dimensions and operating conditions of the MH. The projected MH will be equipped with a coaxial rotor system, with rotor disks approximately 3.94 feet in diameter. However, because of restrictions in MARSWIT test section dimensions, the largest testable rotor was limited to 3.33 feet in diameter, approximately 0.65 feet smaller than what will be installed on the MH. In addition to rotor diameter, the selected rotor was chosen to be operational up to 3000 RPM to match the RPM and hover tip Mach Number of the proposed MH.

The selected rotor is highly twisted and defined by the manufacturer as 40x22. The first number represents the rotor diameter in inches. The second number refers to the forward distance traversed, in inches, for every rotor revolution when acting as a propeller [7].

The Siemens Electric AC Motor, model #1FT5104-0AF71-I, was used for rotor operation. This motor was selected for the first-ever Martian atmosphere rotor hover testing in 2002, which also took place in the PAL near-vacuum chamber [8]. Because this motor was proven to successfully operate extensively under vacuum, it was chosen again for this test. Measurements included RPM based on a motor encoder and torque based on motor current; both RPM and torque were

recorded by the Data Acquisition System (DAS). A thermocouple was mounted to the motor for motor temperature monitoring.

An Omron #E3S-AR11 infrared (IR) sensor was used during testing. This is a built-in amplifier photoelectric feedback sensor, which was used to indicate motor RPM. Reflective tape, adhered to the motor shaft, reflects the IR signal once per motor revolution. This sensor was only used to monitor RPM while testing and was not recorded.

To measure rotor thrust, the motor is fixed to three Sensortronics S-Beam load cells, model #60001. Each load cell is single axis and can measure up to 50 pounds within a safe margin. The collective 150-pound measurable weight is required to accommodate the dead weight of the motor and rotor hardware. The load cells were mounted 120 degrees apart about the rotor's axis of rotation.

At 1 atmosphere, rotor thrust is much larger than that at reduced pressure. As the PAL is evacuated to Martian pressures, the atmospheric density within the chamber is approximately 100 times lower than at 1 atmosphere. Consequently, the load cells are operating at their minimum specifications when measuring thrust at extremely low chamber pressures.

MARSWIT wind speed is determined from a 1-millibar (Barocel-590) and a ±1.25-millibar (Setra 239) differential pressure transducer attached to a pitot-static probe, located forward of the test section. The transducer, a model Barocell-590, was on a heated plate located in the PAL control room to minimize temperature drift and was only used for 1-atmosphere measurements. Wind speed is measured only in the direction of air entering the MARSWIT inlet. Moreover, when the atmospheric pressures were different from 1 atmosphere, wind speed was only collected for the two-bladed rotor.

To determine the test hardware structural resonance, a resonant frequency test was performed for each rotor configuration. Within the maximum testable range of 3400 RPM, frequencies with the highest amplitude occur around 1900 RPM for both the two- and four-bladed rotor configurations.

Vibrations were monitored throughout testing by two uniaxial 5g Kistler accelerometers mounted 90 degrees of relative rotation between each other, on a plane perpendicular to the axis of rotation. Accelerometer installation was for the sole purpose of monitoring amplitude throughout testing, particularly around determined resonant frequencies.

Acoustics measurements (not presented in this paper) were taken by microphones placed in the vacuum chamber. The microphones and amplifiers are part of a G.R.A.S. Sound & Vibration System.

Absolute chamber pressure, density, humidity, and temperature sensors located in the PAL vacuum chamber were used for this test. The Setra 204 absolute pressure transducer was used to measure chamber pressure for pressures ranging from 1 atmosphere to around 5.5 millibars. In addition, the Wallace and Tiernan FA129 absolute pressure gauge was used just to indicate absolute pressures of the same range as the Setra 204. One MKS Baratron 127AA 0–13-millibar

absolute pressure transducer was used when low pressures were reached. Lastly, humidity and temperature were measured by a Vaisala DMP248 dewpoint transmitter.

Data Collection

All sensor cables bridge the vacuum chamber wall to the PAL control room, where they are recorded to one of two data systems, an AstroMed Dash 18X (AstroMed) and a PAL LabVIEW system. The AstroMed is a 14-bit DAS used for real-time monitoring and data recording, with real-time sensor calibration and filter application. Rotor thrust, RPM, power, torque, wind speed, acoustics, and stand vibration were recorded to this system. The PAL LabVIEW system recorded absolute chamber pressure, density, humidity, and temperature. In addition to the PAL digital readout of chamber pressure, pressure was also manually recorded from the Wallace and Tiernan FA129 absolute pressure gauge.

POST-PROCESSING

Post-processed data records are merged based on the time stamp of each DAS described prior. Once merged, the data undergoes zero-point subtraction of load cell weight and torque. Periodic zero-point subtraction became particularly important when measuring rotor thrust, as the three load cells demonstrated drift during extended operation; routine zero-points helped capture and mitigate this behavior. In addition to zero-point subtraction, a rotor hub torque tare was applied.

Data Acquisition

There were three data acquisition sources used during the test: an Astro-Med Dash-18 was used to acquire measurements of model instrumentation; an N242 facility data system was used to acquire facility measurements; and a manually recorded run log was used to record model configuration and select facility measurement values, as well as notes about recorded points when needed. The Astro-Med Dash-18 internally processes the acquired data signals to save data in engineering units rather than as voltages, while the N242 facility data system contains both files in engineering units and voltages.

The Astro-Med Dash-18 was set to record channels simultaneously at two different sampling rates, a standard and slow rate. The standard rate was either 200 Hz or 100,000 Hz, and the slow rate was either 100 Hz or 200 Hz, respectively. The 100,000-Hz rate was used to support acoustic measurements. The N242 resident data system recorded data at approximately 3 Hz.

The N242 facility data system and the Astro-Med Dash-18 were independent systems with independent operators. The only synchronization between the systems was that the operators would initiate dataset recording at the same time based on a verbal cue. Data file names for the two systems were also independent, so correlation between data sets was determined by log records of the initial and ending N242 dataset file names in a run and by comparing time stamps of the dataset files from both systems. Although the N242 resident data system was always operational for monitoring facility conditions, datasets were not always acquired for each record point acquired by the Astro-Med Dash-18. For record points missing an N242 dataset, the run log was used to provide tunnel conditions.

Data was acquired for a predetermined series of runs with points for specific model and facility settings. However, since tests always have run-time issues, some of the points had to be repeated and some additional data record points were acquired that did not have point numbers assigned. To allow for easy identification of individual point datasets, each dataset was assigned a unique run and sequence number pair. The run number was same as specified in the run log, but the sequence numbers were based on the ordinal sequence in which the point datasets were acquired. For clarity, the final run and sequence numbers presented in this report have been renumbered.

Initial Post-Processing

The datasets acquired from the N242 facility data system and the Astro-Med Dash-18 contain time histories of their measurement channels. The first step in post-processing is to read all of the time history datasets from both systems and create summary databases where each row contains the means and standard deviations for each channel; a file name of the point dataset and its time stamp for each data point follow next. The information from the run logs is read in from Excel spreadsheets created for each log and used to create a single, combined log table. A log configuration file is used in this process to resolve formatting and column name differences between the individual logs.

Run and point numbers are used to match log data and Astro-Med Dash-18 data. The N242 facility data system uses a different numbering scheme, so time stamps are used to match N242 system points with Astro-Med points. A dry run is performed to sync the three databases to determine if there are problems that need to be corrected. The most common problem is inconsistencies in the logs, which are managed by editing the logs to resolve them. Only data means and standard deviations are included in the merged database.

Zero Corrections

Zero record points were taken before and after each run and RPM sweep. Moreover, to further counteract temperature and recirculation effects, there are sets of runs in which, in addition to taking a zero before and after each RPM sweep, a zero point was taken in between each RPM measurement.

The purpose of a “zero” record point is to determine the change in measurement values from values obtained at a reference condition, which is currently defined as zero tunnel wind speed and zero rotor RPM. For selected measurements, the zero value is subtracted from all measurements obtained during the run in which the zero was recorded and for subsequent runs if no new zeros were obtained. Three types of zero corrections are used depending on the availability of zero and static points: “beginning” zero corrections in which the values for a zero/static point are subtracted from subsequent points, “ending” zero corrections in which the values for a zero/static point are subtracted from previous points, and “both” zero corrections in which the interpolated values from beginning and ending zero/static points are subtracted from points taken in between. The interpolation is based the data point record time.

Weight Tares

Weight tares are the changes in loads measured by loads cells due to shifting weight of the model as the angle is changed in the absence of aerodynamic forces. Measurements of these tares, after zero corrections were made, are presented in Figure 8. As expected, the number of props installed does make a small difference on the magnitude tare loads. Load cell 3 is located on the pivot axis (see Figure 12), resulting in somewhat higher noise levels. The load cell force measurement has estimated tare force subtracted after the zero corrections are applied. The tare estimates are made using the fit equation: Tare = S1∗(1.0−cos(α) + S2∗sin(α). The coefficients for the load cell curve fits and the fit standard deviations are presented in Table 1.

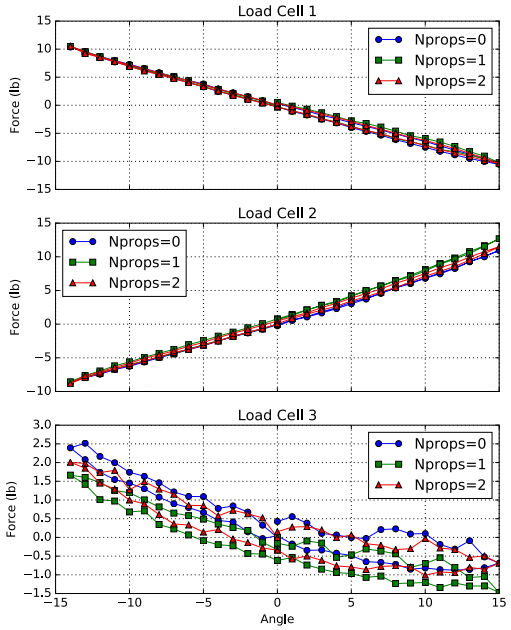

Figure 8. Weight tare values for load cells 1, 2, and 3.

Table 1. Weight tare fit coefficients with standard deviations.

Nprops	Load Cell	S1	S2	Sigma (lb)
0	1	11.99386754	–40.13675701	0.358695099
0	2	27.11330234	37.90820162	0.131569142
0	3	33.50985781	–6.215704452	0.318109694
1	1	17.06010815	–39.7085289	0.403321397
1	2	65.84885034	40.32774456	0.441892038
1	3	0	–5.495353688	0.333470585
2	1	10.07770625	–40.08493139	0.339950515
2	2	41.14243824	38.40839435	0.300244256
2	3	22.76007772	–5.412475948	0.319728605

This weight tare fit is not applied when the angle of the zero record point is the same as the point being analyzed. All data presented in this report was collected at an angle of –14 degrees. Therefore, this weight tare fit is not applied to the presented data.

Aerodynamic Tares

Corrections for aerodynamic tares were considered. These were forces on the model that occur with positive wind speed and no props installed. Two characteristics were expected: first, that the tares should be proportional to dynamic pressure, and second, that the tare forces should have some symmetry about the 0-degree tilt angle. Neither of these expectations seemed evident in the data, so it may be that the tare forces were masked by data scatter. It was therefore decided not to calculate and apply aerodynamic tares at this time.

Torque Tares

After zero corrections and weight tare corrections, torque tares were considered. The torque required to spin the motor with no propellers installed was monitored throughout the RPM range and for 1 atmosphere and reduced pressures. As an improvement to the previous data report [1], an improved torque tare was applied to the experimental data herein.

In addition, at 1-atmosphere data collection, points were collected to up to 200 millibars when the propellers were spinning and the pressure changed at a rate of less than 1 millibar per minute. Further, when the rotors were at reduced pressures, they were spun at higher RPMs than when they were at 1 atmosphere. Therefore, two sets of torque tares (see Figure 9 and Figure 10) were created to cover the range of tested RPM at 1 atmosphere and at reduced pressures.

Absolute Pressure Offset Correction

The Setra 204 was used to record absolute pressure from 1 atmosphere down to 5.5 millibars, and this measurement is part of the recorded data in the N242 system. It was identified that this measurement required a correction in the offset of its calibration. Since this setting could not be directly changed in the N242 system, this offset was instead corrected in the data post-processing.

A Mensor CPC6000 automated pressure calibrator [9] was used to find the corresponding offset. The automated pressure calibrator was connected to the Setra 204, and multiple points were collected ranging from 1 atmosphere to reduced testing pressures comparable to those seen in testing. The difference between the Setra 204 and the automated pressure calibrator readings was fairly constant within this range (see Table 2 and Figure 11). Therefore, the average of all of these readings was calculated and subtracted from the Setra 204 readings.

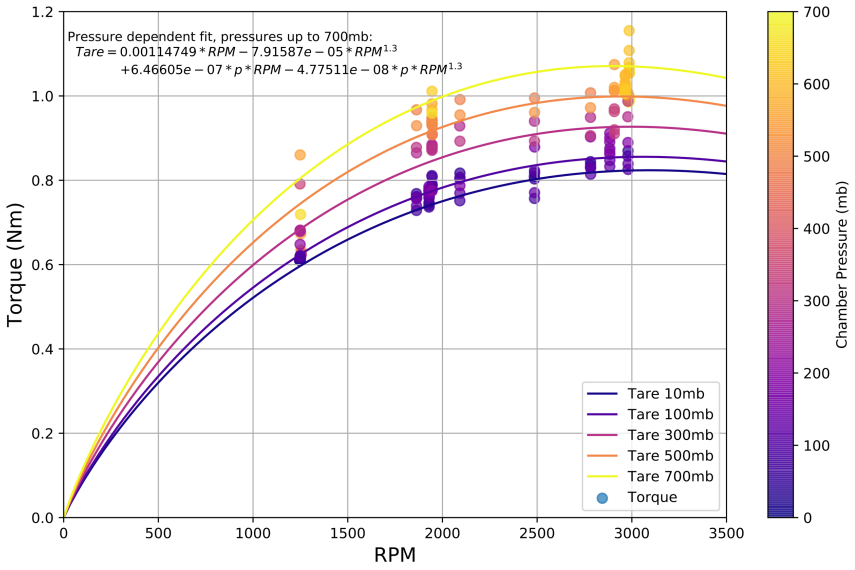

Figure 9. Torque tares at reduced pressures.

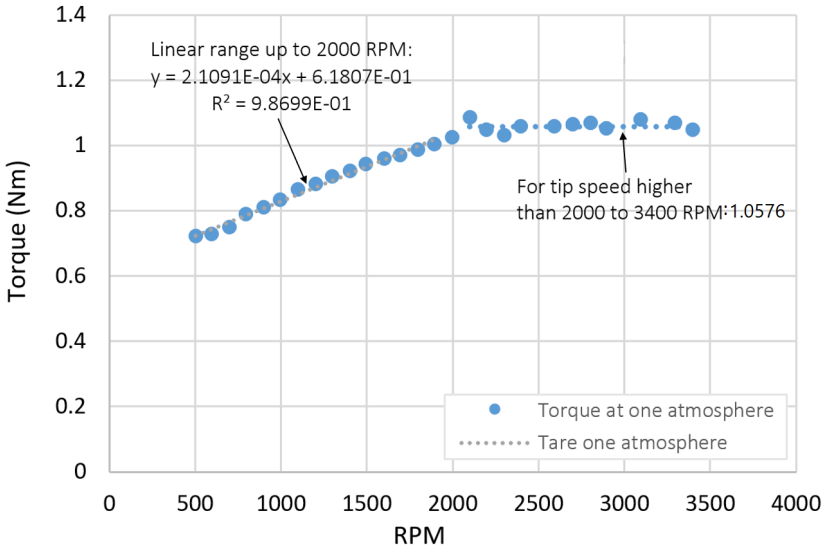

Figure 10. Torque tares at 1 atmosphere.

Table 2. Readings of automated pressure calibrator vs. Setra 204.

Automated Pressure Calibrator (mbar)	Setra 204 (mbar)	Offset (mbar)
11.990	18.666	6.676
12.000	18.658	6.658
14.050	20.773	6.723
14.060	20.781	6.721
20.020	26.774	6.754
20.020	26.779	6.759
29.990	36.731	6.741
40.000	46.687	6.687
60.000	66.627	6.627
100.300	106.903	6.603
100.450	107.033	6.583
200.000	206.583	6.583
303.000	309.553	6.553
404.900	411.573	6.673
404.990	411.615	6.625
606.690	613.452	6.762
606.720	613.482	6.762
699.800	706.526	6.726
749.990	756.656	6.666
800.220	806.813	6.593
801.210	807.837	6.627
850.150	856.648	6.498
899.730	906.088	6.358
997.650	1004.269	6.619
1021.020	1027.692	6.672
	Average:	**6.650**

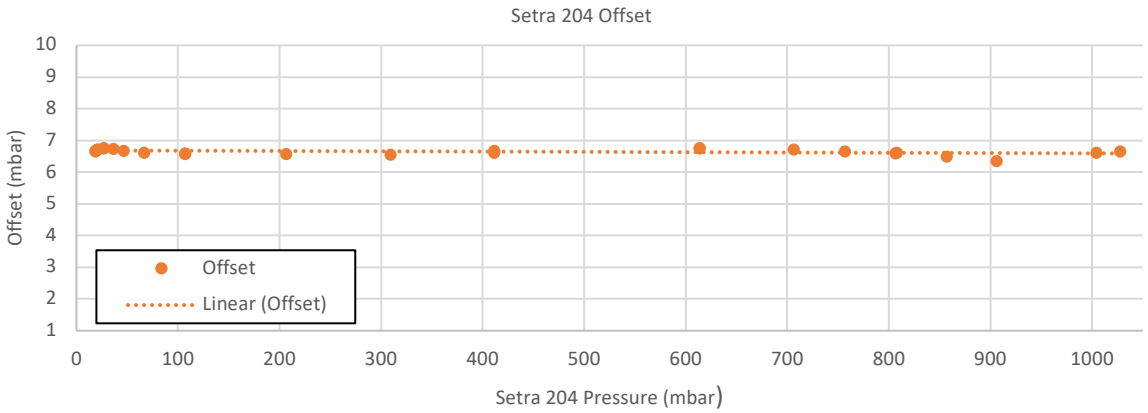

Figure 11. Setra 204 offset vs. pressure.

Force and Moment Calculations

The helicopter test apparatus is mounted on three vertically oriented load cells, positioned as shown in Figure 12. The bolt holes for the load cells are on a circle with a radius of 5.455 inches, that is normal to and centered along the rotor's shaft axis. The load cells are mounted below the model and remain perpendicular to the shaft axis as the model is rotated in pitch. Negative shaft angle is defined as tilting the shaft into the wind.

The load cells read positive in tension, which is confirmed by the recorded weight tares that show load cell #1 having a more positive reading when the pitch is at –14 degrees (tilted into the wind) and load cell #2 having a more negative reading at that pitch angle (see Figure 8). It should be noted that moment values include contributions from side force and drag due to their application occurring at a point several inches above the load cells. It is not possible to remove these contributions since there are no measurements of side force or drag.

Rotor Configurations

Figure 13 shows the rotor in nominal forward flight, thrusting-up configuration. All sign conventions are the same for both configurations, except for torque, which is positive for all positive RPMs.

The presented sign conventions and definitions are in association with a rotor thrusting up and can be applied to all data presented in this report. The angle of attack of the rotor disk, or equivalently, the geometric shaft angle, is defined such that the rotor disk is at 0 degrees when horizontal. When the front of the disk (facing upstream) pitches upwards, the angle of attack is increased, effectively pointing the thrust vector more downstream. All data presented in this report was performed at –14 degrees geometric shaft angle, so the thrust vector points partially upstream. The positive axis directions and resulting positive moment directions are illustrated in Figure 13.

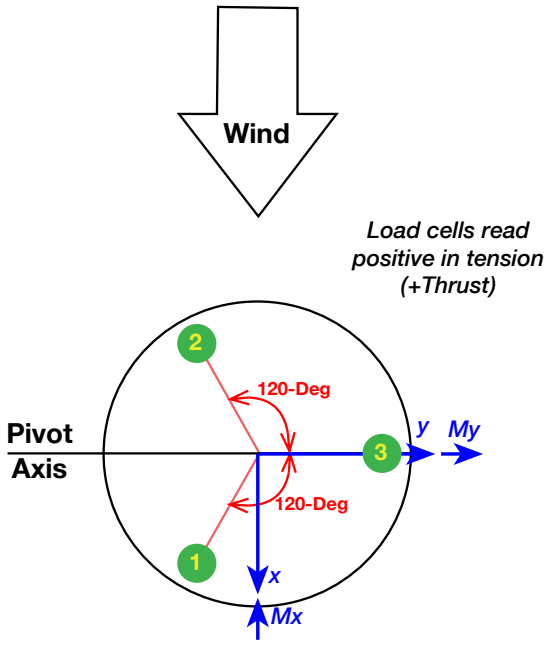

Figure 12. Load cell locations. Bolt holes are on a radius of 5.455 inches.

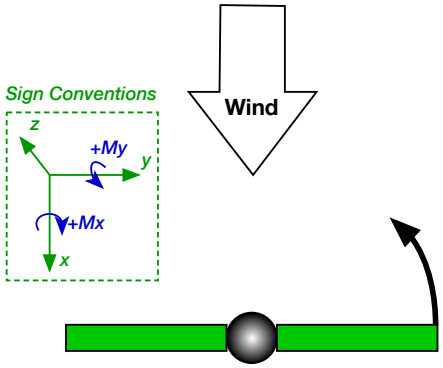

Figure 13. Rotor thrusting up in forward flight, view from ceiling.

Azimuth angle of thrust vector location, φ, is obtained by calculating the angle between the Mx and My components, measured counterclockwise from 0-degree azimuth.

Drag and Side Force Contributions to Measured Moments

The load cells are aligned with the rotor shaft, so in the body-axis system they measure thrust, but no component of either drag or side force. However, drag will contribute to measured pitch moments, My, and side force will contribute to measured roll moments, Mx. Since there are no measurements of drag and side force, their contributions to pitch and roll moments can only be estimated using analytic or computational predictions of drag and side force. The rotor in nominal forward flight is shown in Figure 14 with the drag force vector shown in the body axis system. This shows that the contribution to pitching moment, My, due to drag is D * ZD, where D is the magnitude of the drag and ZD is the moment arm, along the z-axis, from where drag is applied to the centers of the load cells. In a similar manner, side force, S, contributes to the measured rolling moment, Mx. Note that model weight makes no contributions if the data is corrected for zeros and weight tares.

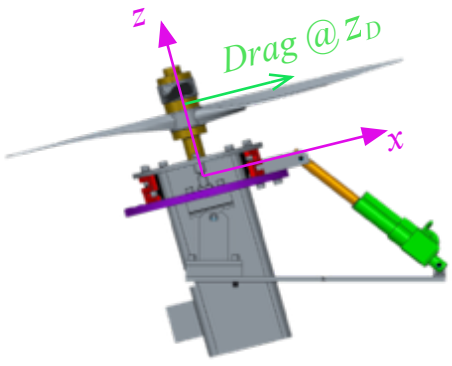

Figure 14. Drag contribution to pitching moment, body-axis system.

PRESENTED DATA

Both two- and four-bladed rotor configurations were tested over a pressure range of 1 bar down to 5 millibars, up to 3400 RPM, and at a fixed forward flight shaft angle of –14 degrees. Atmospheric conditions expected on Mars during the daytime include densities ranging from 0.00087 to 0.00125 lb/ft^3 [10], which are the densities in which the MH is designed to operate [11]. Therefore, pressure was held at values that caused chamber density to be close to the aforementioned range. In addition, the rotors were tested over a pressure range to analyze Reynolds number effect on rotor performance.

Runs 1 to 7 and 37 to 86 incorporated the four-bladed rotor configuration, and runs 8 to 36 incorporated the two-bladed rotor configuration. Table 3 below outlines the categories data can be broken into.

Pressure Decrease

The PAL can evacuate from 1 bar to 5.5 millibars in approximately 45 minutes. Most of the data in this condition was taken without the rotor spinning. However, there was one run in which the two-bladed rotor was run from 2000 to 3400 RPM from 70 to 10 millibars to investigate the flow in the wind tunnel under this condition. The RPM chosen depends on two things. First, it was chosen to avoid test stand resonance determined through Resonance Assessment Profile (RAP) testing. Second, as rotor thrust and vibration is greatest at 1 bar, monitoring of accelerometer and load cell readings limited maximum RPM for safe MARSWIT testing. Table 4 specifies the rotor test conditions.

Table 3. Executed test matrix.

Chamber Test Condition	Test Approach
Pressure Decrease	Pressure decrease from 1 bar down to 5.5 millibars, constant –14-degree rotor shaft angle, wind off, and rotor not spinning. Within this condition there is one run exception where the two-bladed rotor was run from 2000 to 3400 RPM from 70 to 10 millibars.
Constant Pressure	Data in this condition is collected at 1 atmosphere and also when pressure was held at pressures close to the range of expected Martian atmospheric densities during daytime (0.00087 to 0.00125 lb/ft^3 [10]). Data is taken from 0 rotor RPM up to 2100 and 3400 RPM for terrestrial and Mars-like conditions, respectively. Constant –14-degree rotor shaft angle, wind off.
Pressure Drift	Pressure drift at 1 millibar per minute, from 5.5 to 200 millibars, rotor RPM from 0 to 3400 RPM, constant –14-degree rotor shaft angle, wind off.
Pressure Increase	Pressure increase from approximately 200 millibars up to 1 bar, constant RPM, constant –14-degree rotor shaft angle, wind off.

Constant Pressure

Constant pressure can occur at 1 atmosphere and when pressure is held at Mars-like conditions. To decrease pressure, the valve connecting the SVS to the PAL has to be opened. That said, holding constant pressure is currently a challenge in the facility. When reduced pressures are reached, and the PAL is closed off from the SVS, the facility leaks at a rate of roughly 1 millibar per minute. Thus, to hold constant pressure, the facility operator manually regulates the opening of the valve until the desired pressure is steady. However, once manual regulation of the valve ceases, the pressure can deviate up to 5 percent from the steady pressure reached in some instances. Currently, there is no automatic device controlling the valve that can rapidly account for the loss of pressure and set the valve to a desired position without continuous variation.

Two different runs where taken under this condition; a zero RPM point was collected before and after each RPM sweep, and a zero RPM point was taken in between each RPM point. Table 5 shows the range of tested RPM for the two- and four-bladed rotor.

Pressure Drift

If vacuum to the PAL is shut off by the SVS, pressure within the PAL will slowly drift at a rate of 1 millibar per minute. To provide ample data points while minimizing the amount of pressure drift, 15-second data record lengths were collected. As PAL pressure evacuation is dependent on the number of other NASA Ames facilities requiring vacuum, the pressure in which SVS disconnects the PAL from vacuum varied throughout the test program. Reynolds number effects on rotor performance were investigated during this pressure drift condition. Table 6 shows the range of tested RPM and the test conditions for the two- and four-bladed rotor.

Table 4. Test RPMs for each configuration as PAL pressure was evacuated. The exact pressure the chamber was evacuated to varied throughout testing.

Rotor Configuration	Pressure (millibars)	RPM
Four-bladed	~1000 down to 5.5	0
Two-bladed	~1000 down to 10	0 to 3400

Table 5. Range of tested RPM for two- and four-bladed rotors as pressure was held in the vacuum chamber.

Rotor Configuration	Target Pressure (millibars)	RPM
Two-bladed	~1000	0 to 2100
Four-bladed	~1000	0 to 2000
Two-bladed	11	0 to 3400
Four-bladed	14	0 to 3400

Table 6. Range of tested RPM for each configuration.

Rotor Configuration	Pressure (millibars)	RPM
Two-bladed	11 to 200	0 to 3400
Four-bladed	5.5 to 200	0 to 3400

Table 7. RPM for the four-bladed configuration, as PAL pressure was evacuated.

Rotor Configuration	Pressure (millibars)	RPM
Four-bladed	200 to 1000	1250

Pressure Increase

As pressure was increased, the rotors were not spinning for most of the runs. However, there was one run in which the four-bladed rotor was set to a constant RPM while the pressure increased. Table 7 shows the RPM and the test conditions for the four-bladed rotor.

CONCLUSIONS

Despite the challenges involved in testing at the large difference of atmospheric densities between Earth and Mars, successful rotor testing operations measuring thrust, torque, power, and wind speed were demonstrated in the MARSWIT at Martian atmospheric densities and low speeds. Forward flight rotor performance was measured for a two- and four-bladed rotor at terrestrial and Martian atmospheric density conditions. In addition, Reynolds number effects on rotor performance were analyzed for pressures ranging from 40 to 200 millibars. Repeatability at Mars-like conditions was demonstrated with the two-bladed rotor for thrust, torque, power, and wind speed measurements, where differences between the results exhibited an average of no more than 5 percent. In addition to rotor behavior, rotor-induced wind tunnel velocity was compared from Martian atmospheric densities against results at 1 atmosphere.

Analysis of Reynolds number effects on rotor performance for both rotor configurations made from $2x10^4$ to $9x10^4$ showed that C_T and FM decreased around 26 and 36 percent, respectively. Further, C_T and FM exhibited roughly a second-degree polynomial trend for both rotor configurations when plotted against $Re_{0.75R}$ within this range of Re. Moreover, C_P remained fairly constant, exhibiting variations of no more than 5.5 percent.

FUTURE WORK

Wind Tunnel Construction

A larger low-pressure wind tunnel is currently under construction and will be placed alongside the MARSWIT in the PAL near-vacuum chamber. The new wind tunnel will have an 80-inch cross section, which will decrease tunnel effects when testing rotors approximately 4 feet in diameter. Further, to counteract PAL wind recirculation while chamber pressure is pumping down, additional flow treatment will be added at the wind tunnel inlet.

REFERENCES

[1] G. A. Ament, W. J. F. Koning, and B. N. Perez Perez: Isolated Rotor Forward Flight Testing at Martian Atmospheric Density Data Report, NASA/CR–2018-219736, May 2019.

[2] D. Brown, J. Wendel, and D. C. Agle: Mars Helicopter to Fly on NASA's Next Red Planet Rover Mission. Available: https://www.nasa.gov/press-release/mars-helicopter-to-fly-on-nasa-s-next-red-planet-rover-mission. Accessed: 13-Aug-2018.

[3] W. J. F. Koning, W. Johnson, and B. G. Allan: Generation of Mars Helicopter Rotor Model for Comprehensive Analyses, in *AHS Aeromechanics Design for Transformative Vertical Flight*, 2018.

[4] NASA - Planetary Aeolian Laboratory. Available: https://www.nasa.gov/centers/ames/business/planetary_aeolian_facilities.html. Accessed: 03-Aug-2017.

[5] PAL | The Ronald Greeley Center for Planetary Studies. Available: https://rpif.asu.edu/index.php/pal/. Accessed: 23-Nov-2017.

[6] M. McCoy, A. J. Wadcock, and L. A. Young: Documentation of the Recirculation in a Closed-Chamber Rotor Hover Test, NASA TM-2016-219162, Aug. 2016.

[7] W. J. F. Koning: Generation of Performance Model for the Aeolian Wind Tunnel (AWT) Rotor at Reduced Pressure, NASA CR-2018-219737, Jan. 2018.

[8] L. A. Young and E. W. Aiken: Engineering Studies into Vertical Lift Planetary Aerial Vehicles, in *AHS International Meeting on Advanced Rotorcraft Technology and Life Saving Activities*, Utsunomiya, Tochigi, Japan, 2002.

[9] *CPC6000 Operating Instructions Modular Precision Pressure Controller Operating Instructions-CPC6000,* Mensor, 2016, p. 105.

[10] J. (Bob) Balaram et al.: Mars Helicopter Technology Demonstrator, *AIAA Science and Technology Forum and Exposition (AIAA SciTech),* Kissimmee, FL, 2018.

[11] H. F. Grip et al.: Guidance and Control for a Mars Helicopter, *AIAA Science and Technology Forum and Exposition (AIAA SciTech),* Kissimmee, FL, 2018.

APPENDIX A—ISOLATED ROTOR HARDWARE TECHNICAL DRAWINGS

8 | 7 | 6 | 5 | 4 | 3 | 2 | 1

DRAWING NUMBER A242 TESTSTAND_DATAREPORT | SHEET 1 | REV

REVISIONS

REV	DESCRIPTION	DATE	APPROVAL
B	PART 11 REVISION	8/4/16	GA

NOTES: UNLESS OTHERWISE SPECIFIED

CAD PLATE PER QQ-P-L16 TYPE II, CLASS 2

RELEASED DRAWING

DATE: 7/29/16

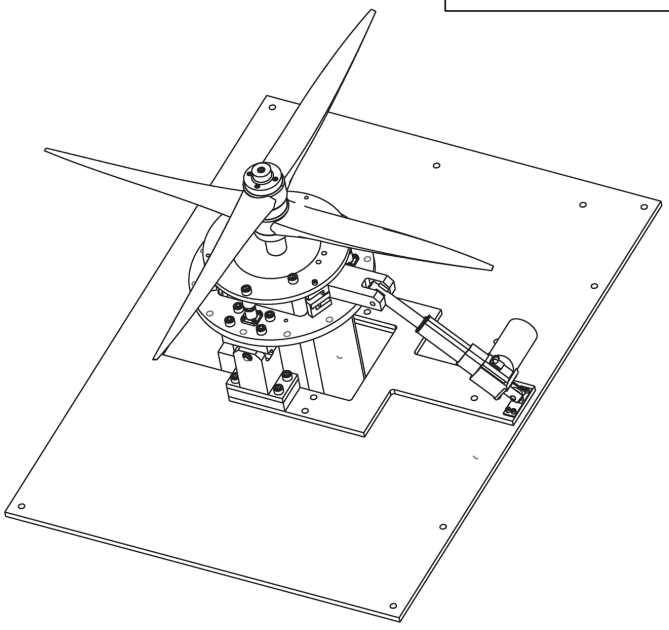

1 242 WIND TUNNEL STAND CONFIG #1 (0-DEG ANGLE)

			23		MCMASTER CARR #91253A375	FLT HD SCREW 82° 0.500-20 UNF X 1.25" LONG	CUSTOMER SUPPLIED BLACK-OXIDE ALLOY STEEL		18
			8		MCMASTER CARR #90044A171	SHCS .500-20 UNF 2.5 LONG	CUSTOMER SUPPLIED BLACK-OXIDE ALLOY STEEL		17
			30		MCMASTER CARR #91251A014	SHCS .500-20 UNF 1.25 LONG	CUSTOMER SUPPLIED BLACK-OXIDE ALLOY STEEL		16
			12		MCMASTER CARR #91253A377	FLT HD SCREW 82° 0.500-20 UNF X 1.5" LONG	CUSTOMER SUPPLIED BLACK-OXIDE ALLOY STEEL		15
			1			MOTOR ASSEMBLY	CUSTOMER SUPPLIED		14
			1			HUB ASSEMBLY	CUSTOMER SUPPLIED		13
			1			LOADCELL SHEAR PIN	SS 15-5 PH 975		12
			1			ACTUATOR SUPPORT BLOCK	A-36 STEEL		11
			1			PA-03 PROGRESSIVE AUTOMATION ACTUATOR	CUSTOMER SUPPLIED		10
			1			ACTUATOR LUG	CUSTOMER SUPPLIED		9
			1			WIND TUNNEL BASE PLATE	A572-STEEL GRADE 50 FTU-65 KSI		8
			1			METRIC PLATE 2	SS 17-4 PH 900		7
			1			METRIC PLATE 1	CUSTOMER SUPPLIED SS 15-5 PH 975		6
			2			HINGESUPPORT LUG	SS 17-4 PH 900		5
			2			HINGESUPPORT CLEVIS	SS 15-5 PH 975		4
			2			HINGESUPPORT MIDPLATE	A-36 STEEL		3
			2			HINGESUPPORT BASE PLATE	A-36 STEEL		2
			X			242 WIND TUNNEL STAND CONFIG #1 0-DEG			1
		-2	-1	CAGE CODE	PART OR IDENTIFYING NO.	DESCRIPTION/NOMENCLATURE	MATERIAL SPECIFICATION	SHEET ZONE	ITEM NO.
QTY REQ'D PER ASSY									

PARTS LIST

		1		MCMASTER CARR #97245A697	CLEVIS PIN WITH COTTER PIN ∅.375, 3 LONG, 2.75 USEABLE	CUSTOMER SUPPLIED ZINC-PLATED STEEL		25
		12		MCMASTER CARR #91251A016	SHCS .25-20 UNF 1.50 LONG	CUSTOMER SUPPLIED BLACK-OXIDE ALLOY STEEL		24
		4		MCMASTER CARR #91251A544	SHCS .25-20 UNF 1.25 LONG	CUSTOMER SUPPLIED BLACK-OXIDE ALLOY STEEL		23
		3			SENSORTRONICS S-BEAM LOAD CELL MODEL 60001 (50 LBS)	CUSTOMER SUPPLIED ALUMINUM		22
		12		MCMASTER CARR #91251A345	SHCS 10-32 THREAD .75 LONG	CUSTOMER SUPPLIED BLACK- OXIDE ALLOY STEEL		21
		3		MCMASTER CARR #5931K76	.500-IN PIN LINEAR BALL BEARING 1.25 LONG	CUSTOMER SUPPLIED SS 440C		20
		2		MCMASTER CARR #93890A192	GROOVED CLEVIS PIN ∅.500 X 3.25 LONG	CUSTOMER SUPPLIED SS 18-8		19
		X			242 WIND TUNNEL STAND CONFIG #1 0-DEG			1

UNLESS OTHERWISE SPECIFIED ALL DIMENSIONS ARE IN INCHES.
ALL DIMENSIONS AND TOLERANCES APPLY AFTER SURFACE TREATMENT.

TOLERANCE UNLESS OTHERWISE SPECIFIED
FRACTIONAL ± /
.X ± 0.1
.XX ± 0.01
.XXX ± 0.001
ANGULAR ± 0.5
DIAMETER ON SAME AXIS TOTAL RUN OUT .XXX
ALL MACHINED SURFACES TO BE XXX ✓

DRILLED HOLE TOLERANCES

DIAMETER	TOLERANCE
.000-.125	+.005-.001
.126-.500	+.010-.002
.501-1.000	+.015-.002
1.001-2.000	+.030-.003
OVER 2.000	+.060-.005

BREAK SHARP CORNERS .XX MAX

DONOTSCALEDRAWING

NO. NEXT ASSEMBLY
APPLICATION

PRELIM RELEASE	DATE	DRAWN G. AMENT	DATE 7/29/16	Ames Research Center Moffett Field, California 94035-1000
INITIAL RELEASE	DATE	CHECKED G. WILLINK	DATE 7/29/16	242 WIND TUNNEL STAND
LATEST REVISION	DATE	DESIGNED G.AMENT H.CUMMINGS	DATE 7/29/16	
PROJECT MGR L. YOUNG	DATE	STRESS	DATE	
SUPERVISOR W. WARMBRODT	DATE	MATERIAL	DATE	
REQUESTOR	DATE	Q.A.	DATE	

SIZE D | CAGE CODE 25307 | REV A
SCALE 0.111 | INDEX DATE | SHEET OF 13
PROE DRAWING FILE NAME: 242_TESTSTAND_DATAREPORT | WC REV:

8 | 7 | 6 | 5 | 4 | 3 | 2

8	7	6	5	4	3	2	1

A242 DRAWING NUMBER: TESTSTAND_DATAREPORT | SHEET 1 REV: 2

RELEASED DRAWING

DATE: 7/29/16

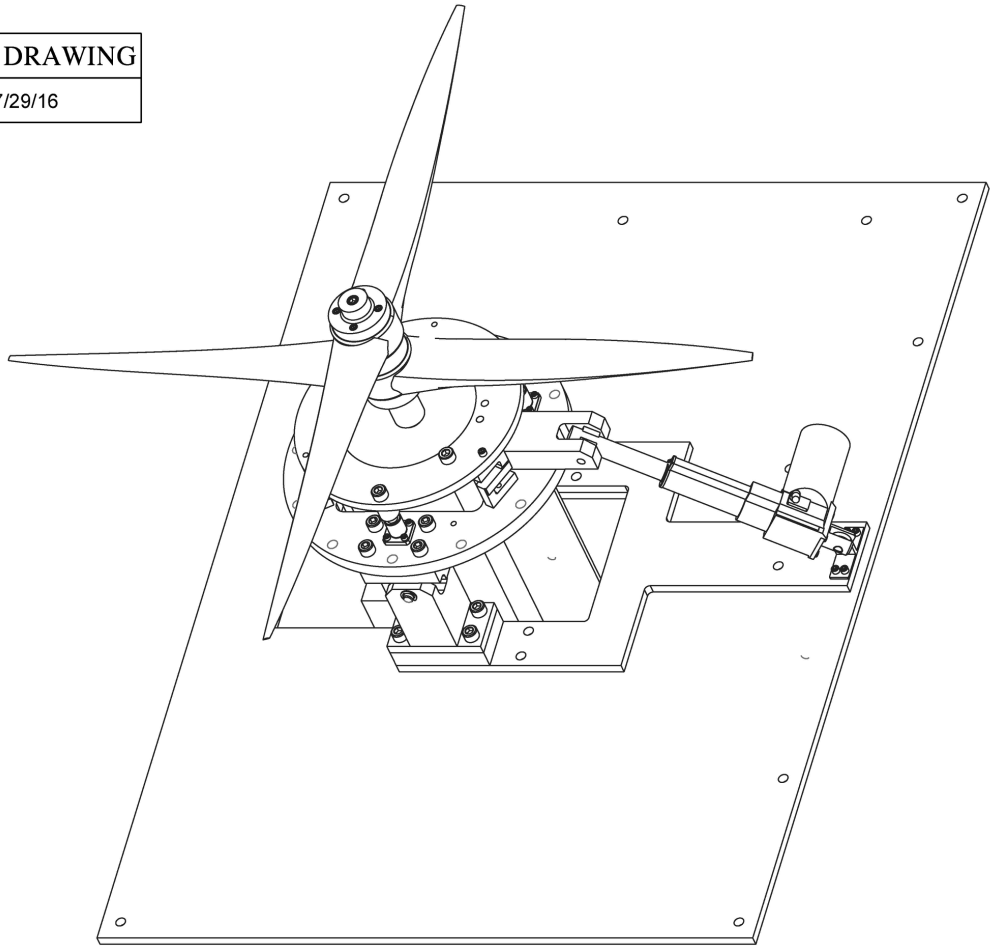

1 242 WIND TUNNEL STAND CONFIG #1 (0-DEG ANGLE)

SEE SHEET ONE FOR REVISIONS

SIZE	CAGE CODE	REV
D	25307	A

242_TESTSTAND_DATAREPORT

SCALE 0.125 | INDEX DATE | SHEET | OF 13

PROVE DRAWING FILE NAME: | WC REV:

242 TESTSTAND_DATAREPORT

8	7	6	5	4	3	2	1

RELEASED DRAWING

DATE: 7/29/16

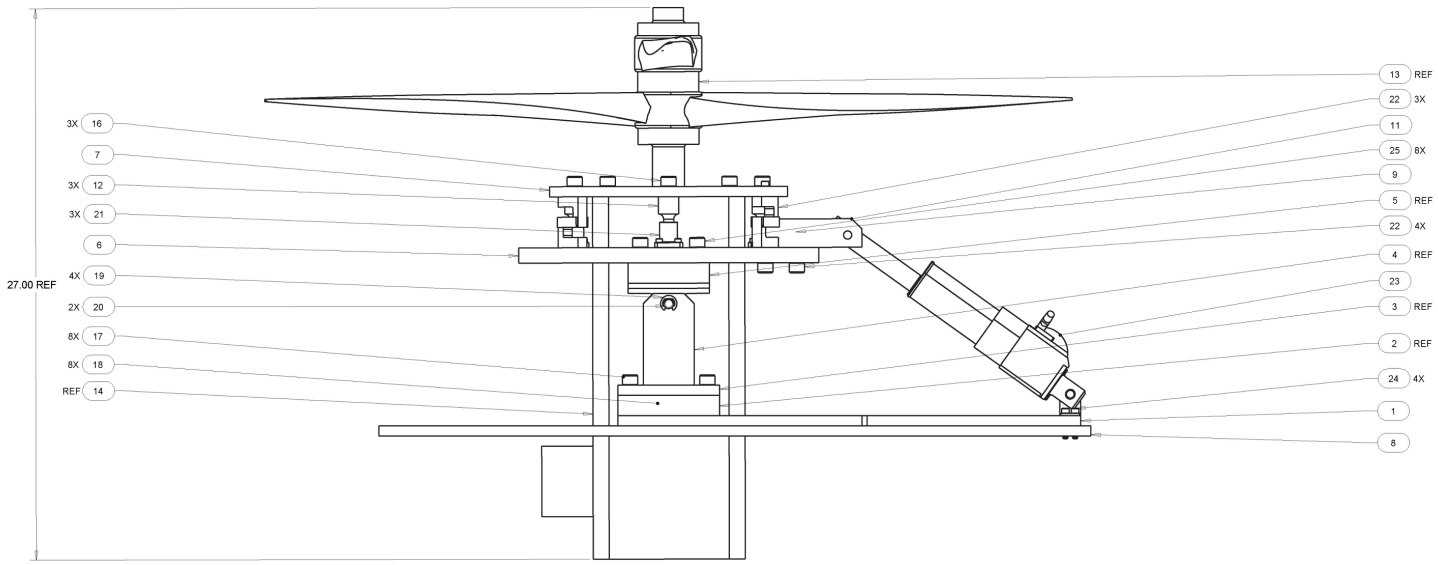

1 242 WIND TUNNEL STAND CONFIG #1 (0-DEG ANGLE)

SEE SHEET ONE FOR REVISIONS

SIZE	CAGE CODE	REV
D	25307	A

242_TESTSTAND_DATAREPORT

SCALE 0.111 | INDEX DATE | SHEET | OF 13

PROVE DRAWING FILE NAME: | WC REV:

242_TESTSTAND_DATAREPORT

RELEASED DRAWING

DATE: 7/29/16

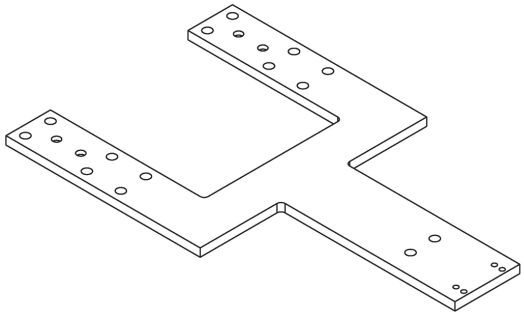

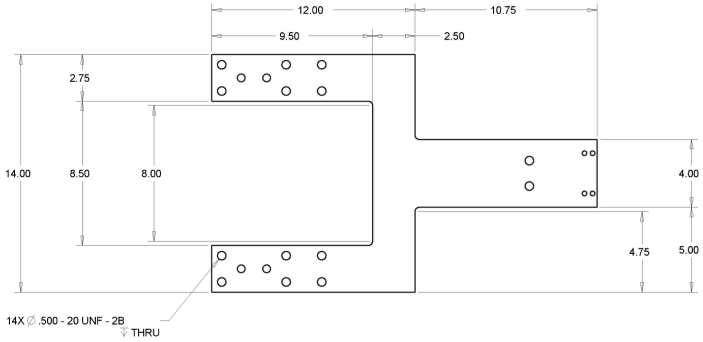

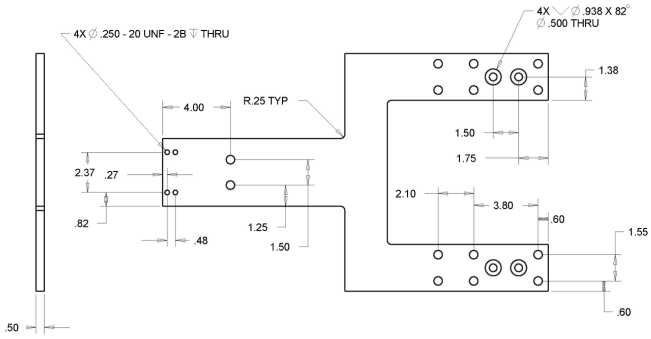

1 ACTUATOR BASE PLATE

SEE SHEET ONE FOR REVISIONS

SIZE	CAGE CODE	REV
D	25307	A

SCALE 0.250 | INDEX DATE | SHEET | OF 13

PROVE DRAWING FILE NAME: TESTSTAND_DATAREPORT | WC REV:

RELEASED DRAWING

DATE: 7/29/16

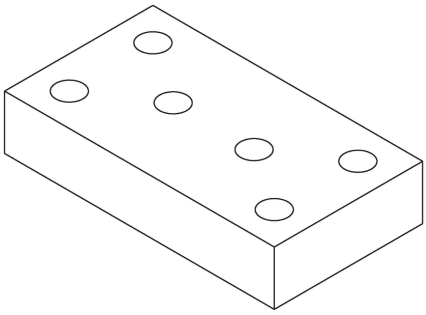

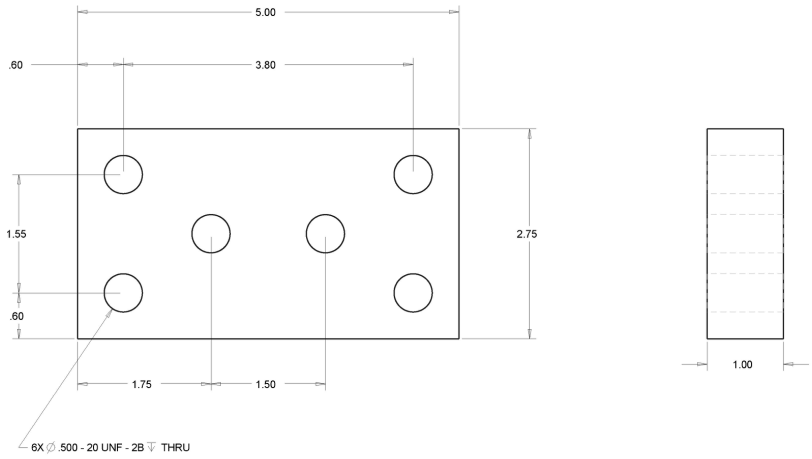

2 HINGESUPPORT BASE PLATE

SEE SHEET ONE FOR REVISIONS

SIZE	CAGE CODE		REV
D	25307	242_TESTSTAND_DATAREPORT	A
SCALE 0.333		INDEX DATE	SHEET OF 13

PROVE DRAWING FILE NAME: TESTSTAND_DATAREPORT WC REV:

RELEASED DRAWING

DATE: 7/29/16

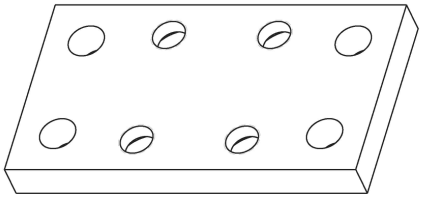

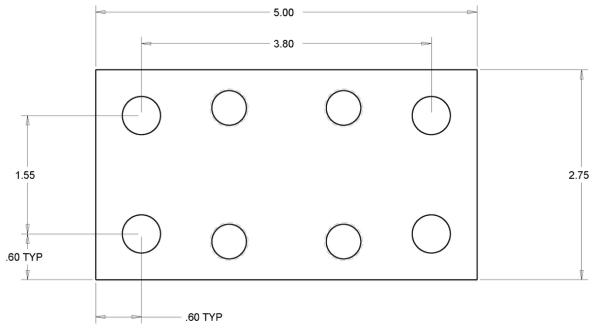

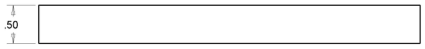

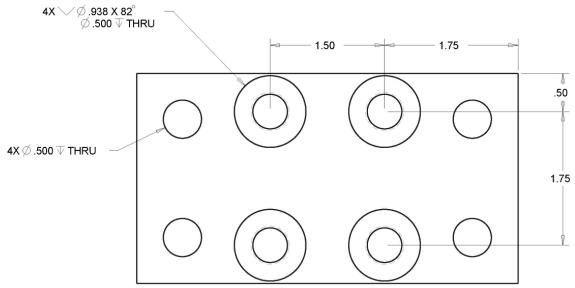

3 HINGESUPPORT MID PLATE

SEE SHEET ONE FOR REVISIONS

SIZE	CAGE CODE		REV
D	25407	TESTSTAND_DATAREP	A
SCALE 0.111	INDEX DATE	SHEET 6 OF 13	

PROVE DRAWING FILE NAME: TESTSTAND_DATAREPORT WC REV:

RELEASED DRAWING

DATE: 7/29/16

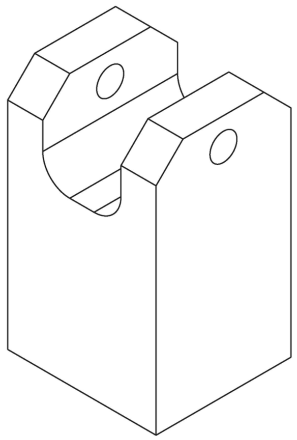

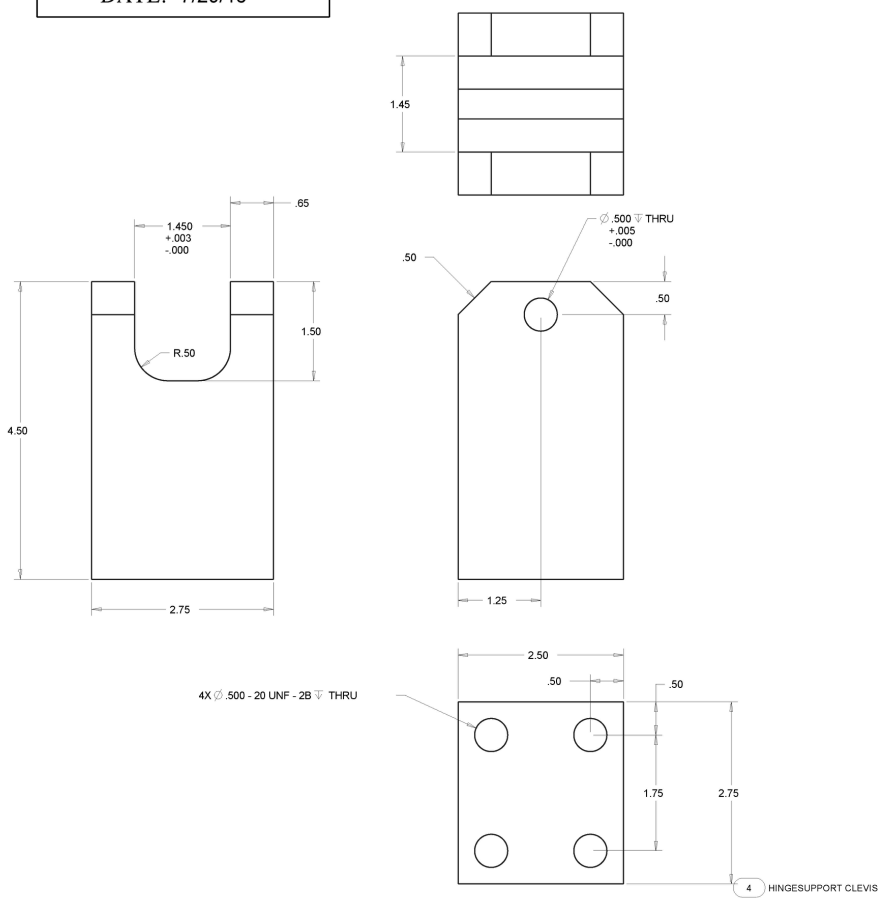

4 HINGESUPPORT CLEVIS

SEE SHEET ONE FOR REVISIONS

SIZE	CAGE CODE	REV
D	25307	A

SCALE 1.000 | INDEX DATE | SHEET | OF 13

PROVE DRAWING FILE NAME: A242_TESTSTAND_DATAREPORT | WC REV:

DRAWING NUMBER: A242 TESTSTAND_DATAREPORT | SHEET 1 REV: B

RELEASED DRAWING

DATE: 7/29/16

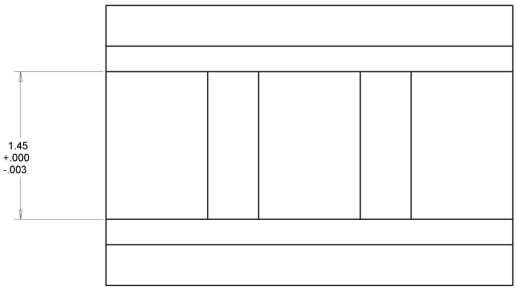

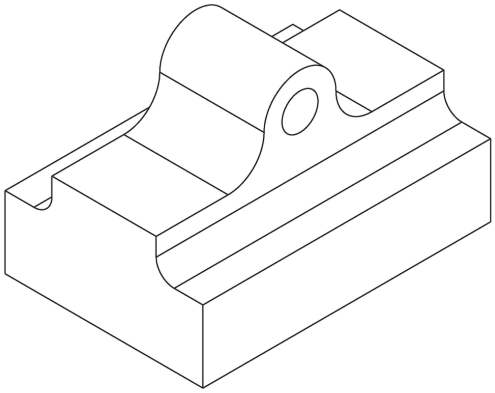

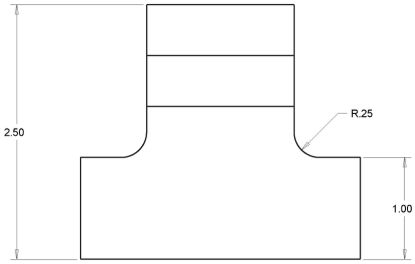

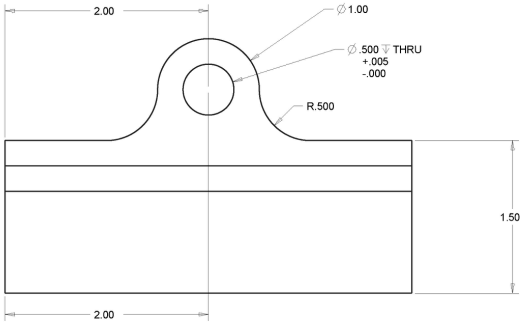

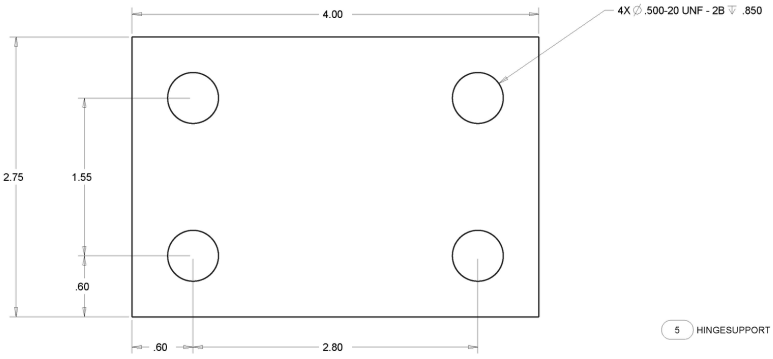

5 HINGESUPPORT LUG

SEE SHEET ONE FOR REVISIONS

SIZE	CAGE CODE	REV
D	25307	A

SCALE 1.000 | INDEX DATE | SHEET 6 OF 13

242 TESTSTAND_DATAREPORT

PROVE DRAWING FILE NAME: | WC REV:

242 TESTSTAND_DATAREPORT

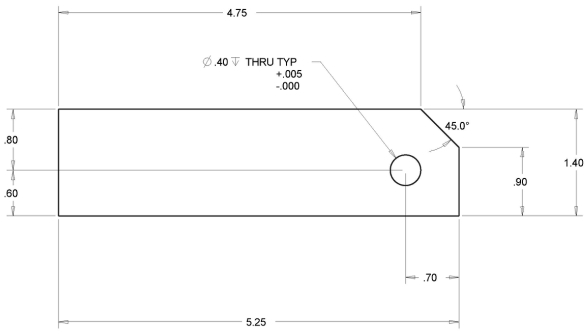

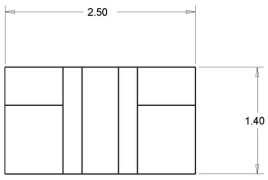

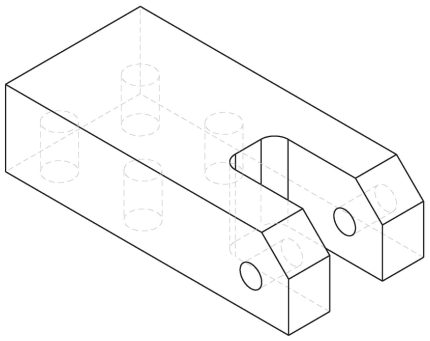

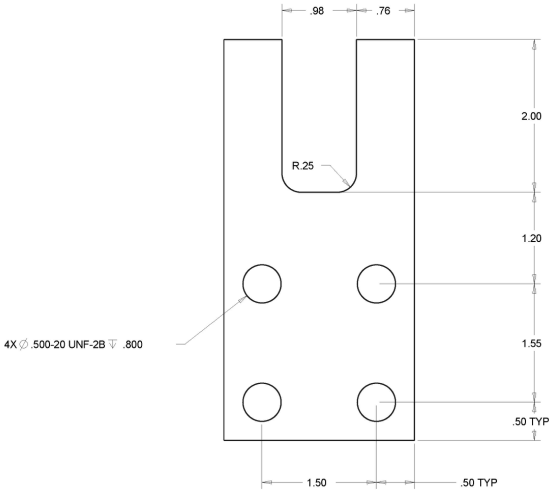

DRAWING REVISION

THIS DRAWING SUPERCEDES ALL PREVIOUS VERSIONS & REVISIONS

REVISION LETTER: B
DATE: 8/5/16
SIGNATURE: G. AMENT

11 ACTUATOR SUPPORT BLOCK

SEE SHEET ONE FOR REVISIONS

SIZE	CAGE CODE	REV
D	25307	A

242_TESTSTAND_DATAREPORT
SCALE 1.000 INDEX DATE SHEET 9 OF 13
PROVE DRAWING FILE NAME: WC REV:
242_TESTSTAND_DATAREPORT

DRAWING NUMBER: A242 TESTSTAND_DATAREPORT | SHEET | REV

REVISIONS

REV	DESCRIPTION	DATE	APPROVAL

DRAWING REVISION

THIS DRAWING SUPERCEDES ALL PREVIOUS VERSIONS & REVISIONS

REVISION LETTER: A
DATE: 8/5/16
SIGNATURE: G. AMENT

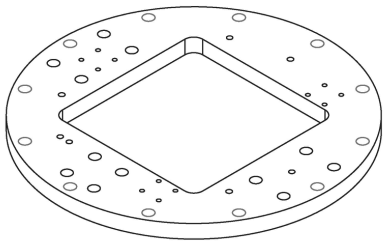

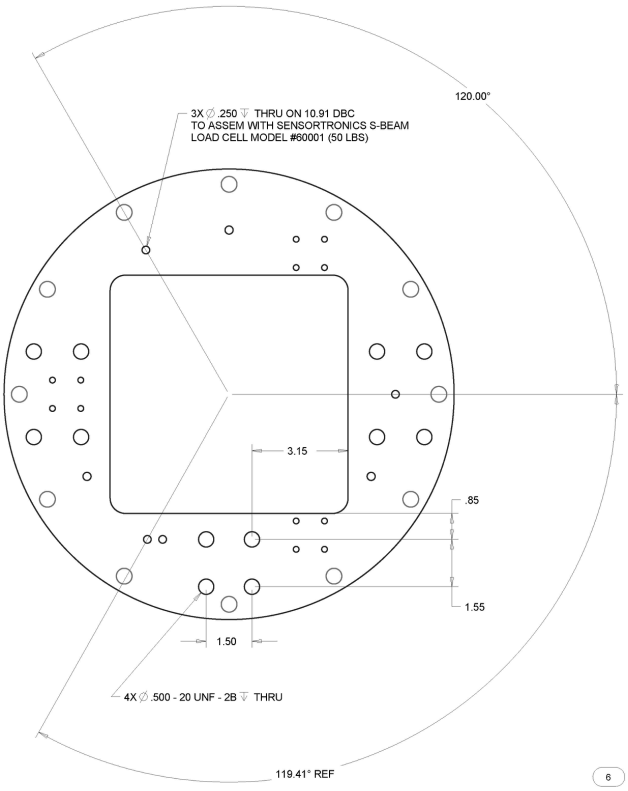

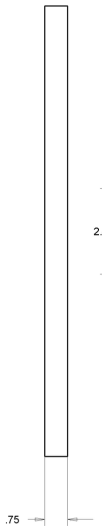

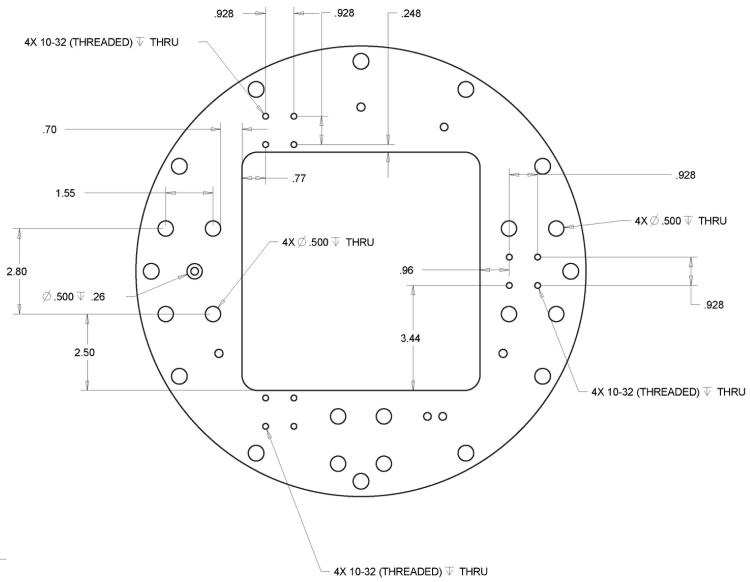

6 METRIC PLATE 1

SEE SHEET ONE FOR REVISIONS

SIZE	CAGE CODE	REV
D	25307	A

SCALE 1.000 | INDEX DATE | SHEET 1 OF 13

PROVE DRAWING FILE NAME: A242_TESTSTAND_DATAREPORT | WC REV:

RELEASED DRAWING

DATE: 7/29/16

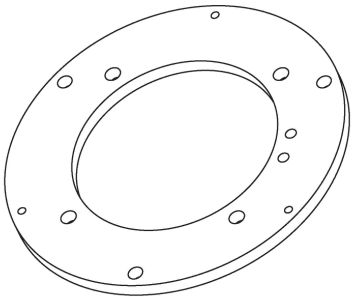

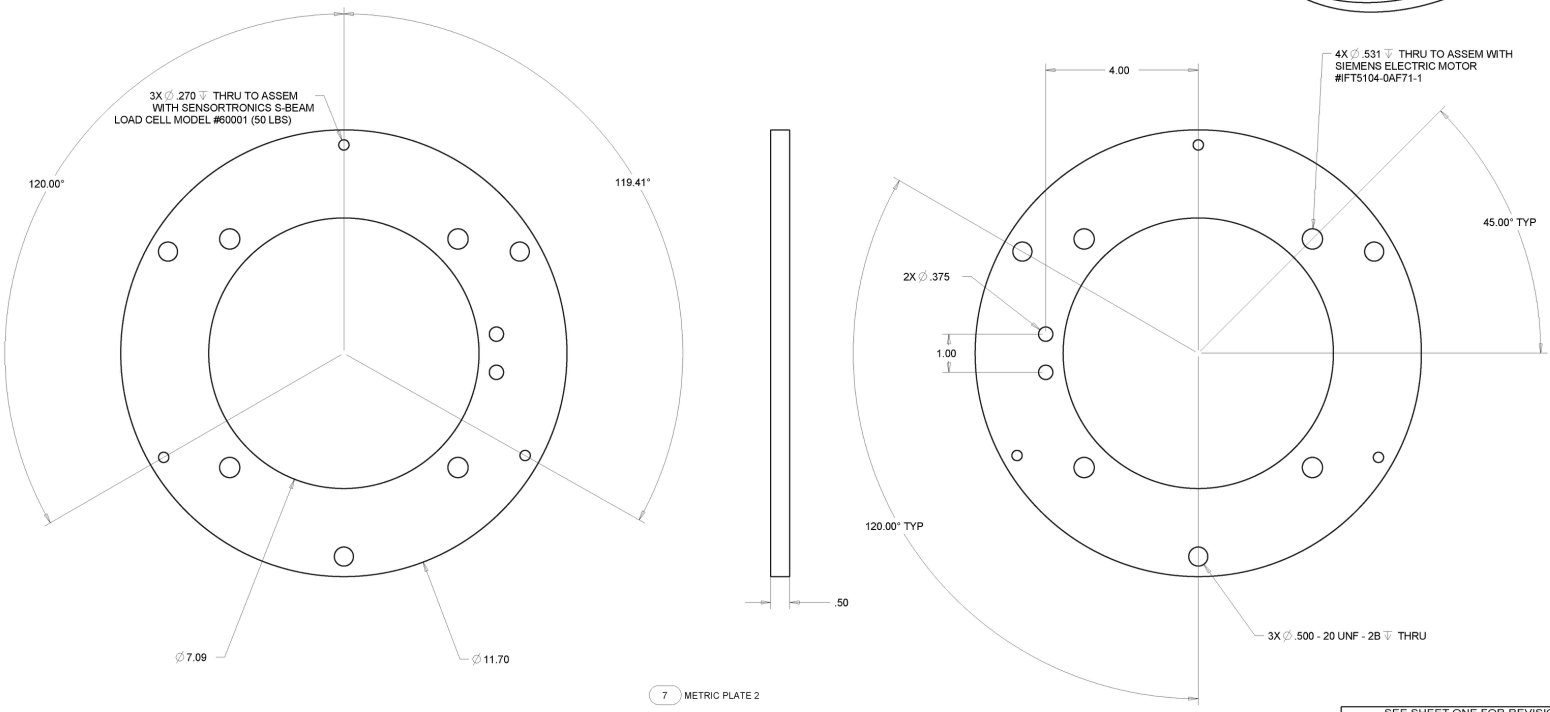

7 METRIC PLATE 2

SEE SHEET ONE FOR REVISIONS

SIZE	CAGE CODE		REV
D	25307	242 TESTSTAND_DATAREPORT	A

SCALE 0.333 | INDEX DATE | SHEET | OF 13

PROVE DRAWING FILE NAME: | WC REV:
242 TESTSTAND_DATAREPORT

MATCH TO ITEM 36 / CHECK FIT
ID TOLERANCE OF .500 SHAFT IS -0.0004" TO 0"

RELEASED DRAWING

DATE: 7/29/16

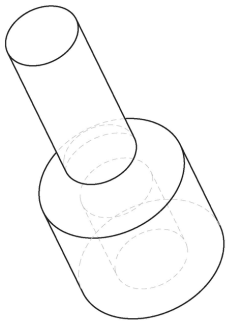

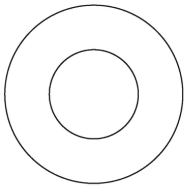

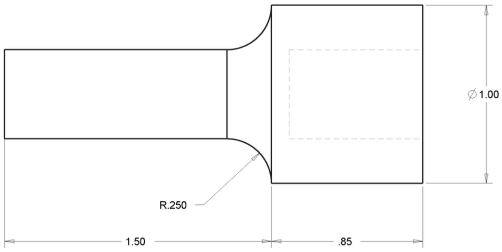

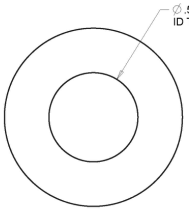

12 LOADCELL SHEAR PIN

SEE SHEET ONE FOR REVISIONS

SIZE	CAGE CODE	REV
D	25307	A

242_TESTSTAND_DATAREPORT

SCALE 0.500 | INDEX DATE | SHEET | ØF 13

PROVE DRAWING FILE NAME: | WC REV:

242 TESTSTAND_DATAREPORT

1 WILL ADD 8 MOUNTING HOLES FOR 4 HANDLES NEAR CORNDERS OF PLATE

RELEASED DRAWING

DATE: 7/29/16

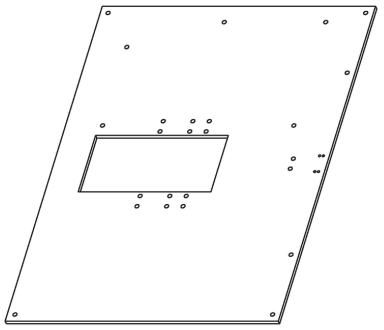

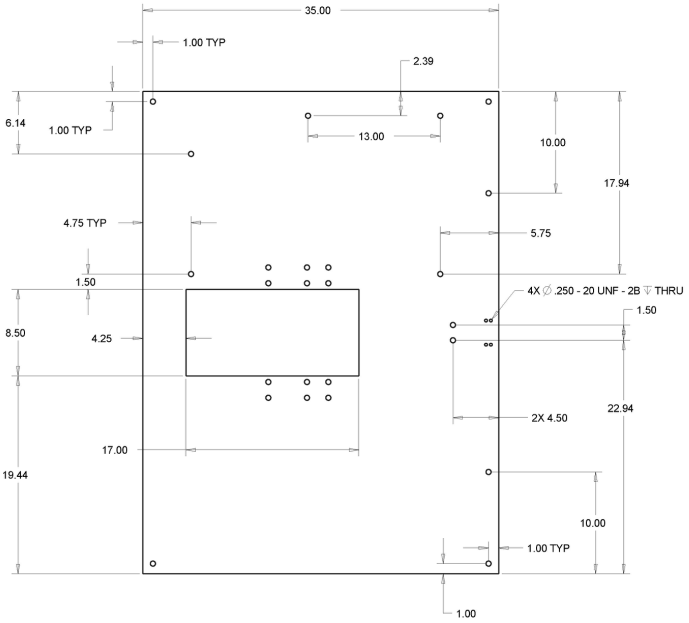

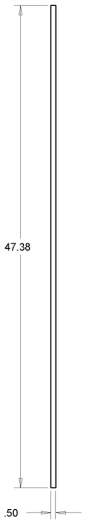

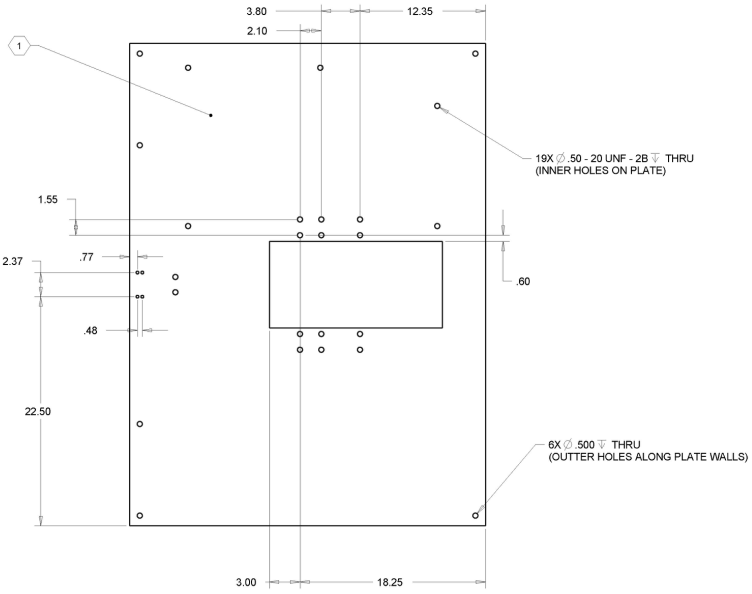

8 WIND TUNNEL BASE PLATE

SEE SHEET ONE FOR REVISIONS

SIZE	CAGE CODE		REV
D	25307	242_TESTSTAND_DATAREPORT	A
SCALE 2.000		INDEX DATE	SHEET 13 OF 13

PRO/E DRAWING FILE NAME: 242_TESTSTAND_DATAREPORT WC REV: